the saturation, and a magnetization value of 1700 emu mol^{-1} G, as experimentally observed, seems to be in good agreement with our hypothesis.

We assume that the dipolar interaction between the chains is the driving force to three-dimensional ferromagnetic order also in $Ni(hfac)_2NITMe$. Qualitatively, the lower transition temperature, compared with the manganese chains, can be explained by the smaller spin of nickel(II) compared to manganese(II), which makes the dipolar interaction less effective. This is also in line with the fact that the analogous copper chain, in which the coupling is much smaller than in the manganese and nickel derivatives and the spin is smaller too, do not undergo any phase transition above 1 K.

In conclusion, in the $M(hfac)_2NITR$ magnetic materials the one-dimensional character is very well preserved by the bulky hfac ligands, which do not provide effective exchange pathways between the metal ions. The strong intrachain antiferromagnetic interactions in the manganese and nickel derivatives build up large uncompensated moments at low temperature in such a way that even the weak interchain dipolar interaction is sufficient to establish three-dimensional order. Therefore the transition temperature could in principle be increased by either increasing the intrachain interaction or decreasing the interchain distance. Increasing the intrachain interaction does not seem to be very probable, because studies on model mononuclear complexes show that J of about 300-400 cm^{-1} is the upper limit, while the interchain interaction can be improved by changing the hfac ligands with others that can transmit more efficiently the exchange interaction. Indeed, we found that $[Mn(pfb)_2]_2NITR$, where pfb is pentafluorobenzoate, orders three-dimensionally above 20 K.[34]

Acknowledgment. The financial support of the Italian Ministry of Public Education and of the CNR is gratefully acknowledged.

Registry No. $Ni(hfac)_2NITMe$, 121269-34-9; $Ni(hfac)_2(NITPh)_2$, 121288-63-9; $Ni(hfac)_2$, 14949-69-0.

Supplementary Material Available: Table SI, listing crystallographic data, Tables SII-SV, listing anisotropic thermal factors, bond distances, bond angles, and calculated positional parameters of hydrogen atoms, and Table SVI, listing least-squares planes and deviations (12 pages); tables of calculated and observed structure factors (14 pages). Ordering information is given on any current masthead page.

---

(34) Caneschi, A.; Gatteschi, D.; Renard, J. P.; Rey, P.; Sessoli, R. *J. Am. Chem. Soc.* **1989**, *111*, 785.

Contribution from the Dipartimento di Chimica Inorganica e Struttura Molecolare, Università di Messina, Salita Sperone, 31, Villaggio S. Agata, I-98100 Messina, Italy, and Dipartimento di Chimica Inorganica, Chimica Fisica e Chimica dei Materiali, Università di Torino, Via P. Giuria, 7, I-10125 Torino, Italy

Bi- and Polynuclear Complexes with Short-Bite Ligands Bridging Metal Atoms. $[(\eta^5\text{-}C_5H_5)Rh(\mu\text{-}CH_3O_2CC_2CO_2CH_3)(\mu\text{-}Ph_2Ppy)Rh(CO)(\mu\text{-}Cl)]_2$: Synthesis, X-ray Crystal Structure, Structural Dynamics, and Reactions with CO and SO_2

Enrico Rotondo,[1a] Sandra Lo Schiavo,[1a] Giuseppe Bruno,[1a] Carmela Grazia Arena,[1a] Roberto Gobetto,[1b] and Felice Faraone*,[1a]

Received November 28, 1988

Treatment of $[(\eta^5\text{-}C_5H_5)Rh(\mu\text{-}CO)(\mu\text{-}Ph_2Ppy)Rh(CO)Cl]$ (1) (Ph_2Ppy = 2-(diphenylphosphino)pyridine) with the activated acetylenes dimethyl acetylenedicarboxylate (DMA) and diethyl acetylenedicarboxylate (DEA), in CH_2Cl_2 solution, yields the tetranuclear complexes $\{[(\eta^5\text{-}C_5H_5)Rh(\mu\text{-}DMA)(\mu\text{-}Ph_2Ppy)Rh(CO)(\mu\text{-}Cl)]_2\cdot CH_2Cl_2\}$ (**2**) and $\{[(\eta^5\text{-}C_5H_5)Rh(\mu\text{-}DEA)(\mu\text{-}Ph_2Ppy)Rh(CO)(\mu\text{-}Cl)]_2\cdot CH_2Cl_2\}$ (**3**), respectively. The alkyne in both the complexes adopts the $\mu\text{-}\eta^2\text{-}\|$ (cis-dimetalated olefinic) bonding mode. The structure of **2** was established by X-ray crystallography: the crystals are triclinic, space group $P\bar{1}$, with a = 11.805 (1) Å, b = 11.791 (1) Å, c = 12.042 (2) Å, α = 98.7 (2)°, β = 108.9 (2)°, γ = 90.2 (2)°, and Z = 2. Least-squares refinement of 381 parameters using 3971 reflections yields R = 0.035 and R_w = 0.036. The molecule shows a crystallographic inversion center originating from the presence of two asymmetrical bridging chloro ligands that link two bimetallic units. Each rhodium dimer unit is completely asymmetrical and consists of two rhodium atoms bridged by the Ph_2Ppy and the DMA ligands. The Rh(1)-Rh(2) bond distance is 2.661 (1) Å and the Rh(1)···Rh(1') separation is 3.900 (1) Å. The structural parameters concerning the inner coordination sphere provide useful information about the formation of the tetranuclear species **2**. Both Rh-Cl distances are somewhat long [Rh(1)-Cl(1) = 2.516 (1) Å, and Rh(1)-Cl(1') = 2.670 (1) Å]. DMA is attached essentially parallel to the Rh(1)-Rh(2) axis in a cis-dimetalated olefinic geometry; the Rh(1)-C(24) and Rh(2)-C(25) bond distances are significantly different (2.022 (5) and 2.040 (4) Å, respectively). $^{31}P\{^1H\}$ and ^1H NMR spectra of **2** in CD_2Cl_2 solution, at different temperatures, indicate the presence of an equilibrium between the tetranuclear, **2**, and the binuclear, $[(\eta^5\text{-}C_5H_5)Rh(\mu\text{-}DMA)(\mu\text{-}Ph_2Ppy)Rh(CO)(Cl)]$ (**4**), species. The unsaturation of the rhodium(II), 16-electron center in **4** seems to be the key to the reactivity of this species, and it accounts for both the formation of the tetranuclear chloro-bridged species **2** and the reactions of **2** with small molecules such as CO and SO_2. The reaction of **2** with CO and SO_2 leads to adducts that could not be isolated owing to the reversibility of the process. ^{31}P, ^1H, and ^{13}C NMR spectra indicate that in these adducts CO and SO_2 are both terminally bonded to rhodium. Hints of a dynamic process involving the formation of acyl derivatives, presumably by insertion of ^{13}CO into the Rh-C(acetylene) bond, are also reported.

Introduction

Previous papers from our laboratories have described the synthesis, and the molecular structure of the symmetric binuclear (η^5-cyclopentadienyl)rhodium complex $[Rh_2(\eta^5\text{-}C_5H_5)_2(\mu\text{-}CO)(\mu\text{-}dppm)]$ (dppm = bis(diphenylphosphino)methane) characterized by the presence of the short-bite dppm as a bridging ligand.[2] This complex contains an electron-rich rhodium-rhodium bond as evidenced by the reactions with H^+, $HgCl_2$, and group 11 atom electrophiles;[3-7] conversely, it does not react with acetylenes, dienes, or alkyl halides. In light of these results and as a part of our interest in the activation of small molecules by bimetallic com-

---

(1) (a) Università di Messina. (b) Università di Torino.

(2) Faraone, F.; Bruno, G.; Lo Schiavo, S.; Bombieri, G. *J. Chem. Soc., Dalton Trans.* **1984**, 533.

(3) Faraone, F.; Lo Schiavo, S.; Bruno, G.; Bombieri, G. *J. Chem. Soc., Chem. Commun.* **1984**, 6.

(4) Bruno, G.; Lo Schiavo, S.; Piraino, P.; Faraone, F. *Organometallics* **1985**, *4*, 1098.

(5) Lo Schiavo, S.; Bruno, G.; Nicolò, F.; Piraino, P.; Faraone, F. *Organometallics* **1985**, *4*, 2091.

(6) Lo Schiavo, S.; Bruno, G.; Piraino, P.; Faraone, F. *Organometallics* **1986**, *5*, 1400.

(7) Bruno, G.; Lo Schiavo, S.; Rotondo, E.; Piraino, P.; Faraone, F. *Organometallics* **1987**, *6*, 2502.

Scheme I

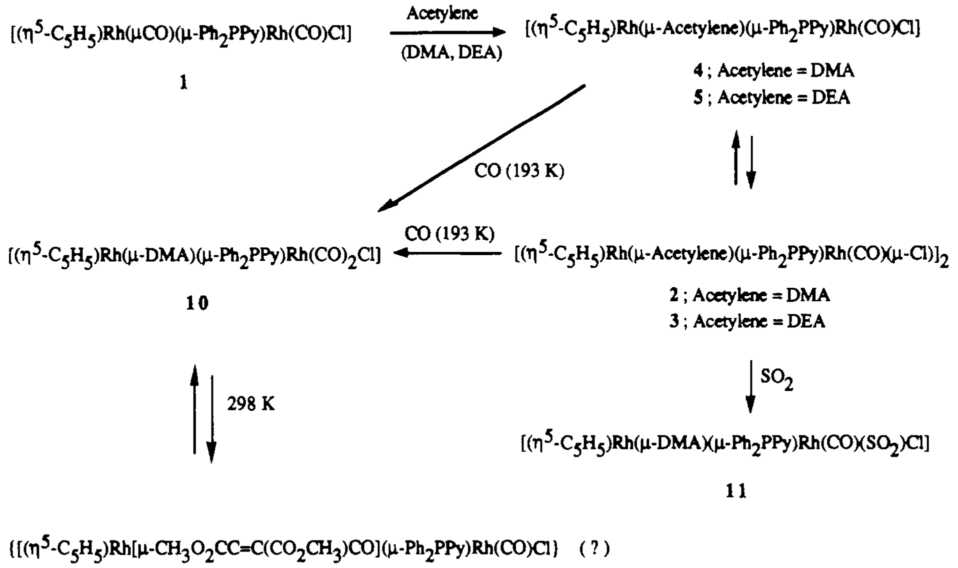

plexes, we have examined the reactions of the unsymmetrically rhodium–rhodium-bonded complex $[(\eta^5\text{-}C_5H_5)Rh(\mu\text{-}CO)(\mu\text{-}Ph_2Ppy)Rh(CO)Cl]$[8] ($Ph_2Ppy$ = 2-(diphenylphosphino)pyridine), with acetylenes. The aim of the present study was also to establish what effects the presence of metals differing in their basicity and coordination number might have on the mode of attachment of the electronegatively substituted acetylenes. An X-ray analysis of the tetranuclear complex $\{[(\eta^5\text{-}C_5H_5)Rh(\mu\text{-}DMA)(\mu\text{-}Ph_2Ppy)Rh(CO)(\mu\text{-}Cl)]_2\cdot CH_2Cl_2\}$ (DMA = dimethyl acetylenedicarboxylate), a representative member of the products, was performed and its behavior in solution studied. One aspect of interest in such a compound is the possibility of insertion of small molecules such as CO and SO_2 into the Rh–acetylene or rhodium–rhodium bond. Such reactions are pertinent to the mechanism of homogeneous carbonylation of alkynes using complexes containing more than one metal center as catalysts.[9-11]

Experimental Section

The compound $[(\eta^5\text{-}C_5H_5)Rh(\mu\text{-}CO)(\mu\text{-}Ph_2Ppy)Rh(CO)Cl]$ (**1**) was prepared as previously described.[8] Other reagents were purchased commercially and used as received. Solvents were dried by standard procedures. IR spectra were recorded as Nujol mulls on KBr plates on a Perkin-Elmer 783 instrument. ^1H, ^{13}C, and ^{31}P NMR spectra were recorded on a Bruker WP80-SY or an JEOL GX-270-89 spectrometer. ^1H and ^{13}C NMR spectra were referenced to internal tetramethylsilane and ^{31}P spectra to external 85% H_3PO_4; positive chemical shifts are for all nuclei to higher frequency. Conductivity measurements were made with a Radiometer CDM 3 conductivity meter. Molecular weights were determined with a Knauer vapor-pressure osmometer. Elemental analyses were performed by Malissa-Reuter Mikroanalytishes Laboratorium, Elbach, West Germany, and by the Microanalytical Laboratory of the Organic Chemistry Institute of Milan.

Preparation of $\{[(\eta^5\text{-}C_5H_5)Rh(\mu\text{-}DMA)(\mu\text{-}Ph_2Ppy)Rh(CO)(\mu\text{-}Cl)]_2\cdot CH_2Cl_2\}$ (2). A dichloromethane solution (50 mL) of $[(\eta^5\text{-}C_5H_5)Rh(\mu\text{-}CO)(\mu\text{-}Ph_2Ppy)Rh(CO)Cl]$ (**1**) (0.120 g, 0.192 mmol) was treated with an excess of DMA (0.030 g, 0.211 mmol), and the resulting mixture was left to stir for ca. 2 h. After this time, the volume of the solvent was reduced to ca. 20 mL and 40 mL of *n*-hexane added, inducing the precipitation of the product as an orange powder. It was filtered, washed with diethyl ether, and dried. Recrystallization from CH_2Cl_2/Et_2O gave **2** as orange crystals (0.138 g, 0.088 mmol), in 92% yield. Anal. Calcd. for $C_{59}H_{52}Cl_4N_2O_{10}P_2Rh_4$: C, 45.29; H, 3.35; Cl, 9.06; N, 1.79. Found: C, 45.38; H, 3.40; Cl, 9.21; N, 1.82. IR (Nujol): ν(CO) 2017, 2020 cm^{-1}; ν_{asym}(CO) 1710, 1690 cm^{-1}. (For the NMR spectra, see Results and Discussion.)

Preparation of $\{[(\eta^5\text{-}C_5H_5)Rh(\mu\text{-}DEA)(\mu\text{-}Ph_2Ppy)Rh(CO)(\mu\text{-}Cl)]_2\cdot CH_2Cl_2\}$ (3). This compound was prepared by following the same procedure used for **2**. Anal. Calcd. for $C_{63}H_{60}Cl_4N_2O_{10}P_2Rh_4$: C, 46.69; H, 3.73; Cl, 8.75; N, 1.73. Found: C, 46.80; H, 3.75; Cl, 8.81; N, 1.75. IR (Nujol): ν(CO) 2020 cm^{-1}; ν_{asym}(CO) 1710, 1690 cm^{-1}.

Reaction of 2 with CO. Carbon monoxide was bubbled for 1 h through a dichloromethane solution (30 mL) of **2** (0.050 g, 0.034 mmol) and the reaction monitored by IR spectroscopy. During this time no color change of the solution was observed, but the IR spectra showed two new bands at 2089 m and 2030 vs cm^{-1}, and a residual absorption at 2017 w cm^{-1}, due to **2**. Owing to the reversibility of the reaction all attempts to isolate a reaction product afforded only the starting material, even when we were operating under CO atmosphere. (For the NMR spectra, see Results and Discussion.)

Reaction of 2 with SO_2. Compound **2** (0.130 g, 0.088 mmol) was dissolved in dichloromethane (30 mL) and SO_2 gas bubbled through the solution. Immediately, the color changed from orange to yellow. SO_2 bubbling was maintained for about 15 min, and then on addition of 40 mL of *n*-hexane, a yellow solid was precipitated. The solvent was evaporated off and the yellow solid washed with diethyl ether and dried under an SO_2 atmosphere. By IR and NMR spectroscopy the yellow solid was identified as $[(\eta^5\text{-}C_5H_5)Rh(\mu\text{-}DMA)(\mu\text{-}Ph_2Ppy)Rh(CO)(SO_2)Cl]$ (**11**). It could not be isolated in an analytically pure form due to release of SO_2, restoring the starting material. IR (Nujol): ν(CO) 2100 cm^{-1}; ν_{asym}(CO) 1710, 1685 cm^{-1}; ν(SO) 1220, 980 cm^{-1}. (For the NMR spectra see Results and Discussion.)

X-ray Data Collection and Structure Refinement. Suitable orange crystals of **2** were obtained by slow evaporation from a dichloromethane–diethyl ether solution. Diffraction measurements were made on a Siemens-Stoe four-circle diffractometer using graphite-monochromated Mo Kα radiation. Accurate unit cell dimensions and crystal orientation matrices were obtained from least-squares refinement of 2θ, ω, and ψ values of 18 strong reflections in the range $15° < 2\theta < 28°$. During the course of the intensity data collection, the crystal showed no loss in intensity. Crystallographic data and other pertinent information are summarized in Table I. Lorentz and polarization corrections were applied to the intensity data, but no absorption correction was made due to the low absorption coefficient. The structure was solved by using standard Patterson methods, successive least-squares refinements, and difference Fourier maps. Anisotropic temperature factors were introduced for all non-hydrogen atoms. Hydrogen atoms were added at calculated positions and included in the structure factor calculations with a common thermal parameter (U = 0.06 Å^2). The weighting scheme used in the last refinement cycles was $w = 2.5107/(\sigma^2F_o + 0.00031F_o^2)$, which showed reasonable consistency in a test of $\omega\Delta^2$ for data sectioned with respect to both F_o and $(\sin\theta)/\lambda$. The models reached convergency with $R = [\sum|F_o| - |F_c|]/\sum|F_o| = 0.035$ and $R_w = [\sum w(|F_o| - |F_c|)^2/\sum w|F_o|^2]^{1/2} = 0.036$. Scattering factors for non-hydrogen atoms were taken from ref 12 and for hydrogen atoms from ref 13. Anomalous

---

(8) Bruno, G.; Lo Schiavo, S.; Rotondo, E.; Arena, C. G.; Faraone, F. *Organometallics* **1989**, *8*, 886.

(9) Pino, P.; Braca, G. In *Organic Synthesis via Metal Carbonyls*; Wender, I., Pino, P., Eds.; Wiley-Interscience: New York, 1977; Vol. II, p 419 and references therein.

(10) (a) Dyke, A. F.; Knox, S. A. R.; Naish, P. J.; Taylor, G. E. *J. Chem. Soc., Dalton Trans.* **1982**, 1297. (b) Burt, R.; Cooke, M.; Green, M. *J. Chem. Soc. A* **1970**, 2981. (c) Dickson, R. S.; Gatehouse, B. M.; Nesbit, M. C.; Pain, G. N. *J. Organomet. Chem.* **1981**, *215*, 97.

(11) Finnimore, S. R.; Knox, S. A. R.; Taylor, G. E. *J. Chem. Soc., Dalton Trans.* **1982**, 1783.

Table I. Crystallographic Data for **2**

formula	$C_{59}H_{52}Cl_4N_2O_{10}P_2Rh_4$	space group	$P\bar{1}$ (No. 2)
a, Å	11.805 (1)	T, °C	21
b, Å	11.791 (2)	λ, Å	0.71069
c, Å	12.042 (3)	ρ_{calcd}, g/cm^3	1.52
α, deg	98.7 (2)	μ, cm^{-1}	12.7
β, deg	96.4 (1)	R	0.035
γ, deg	90.2 (2)	R_w	0.036
V, Å^3	1565.4		
Z	2		

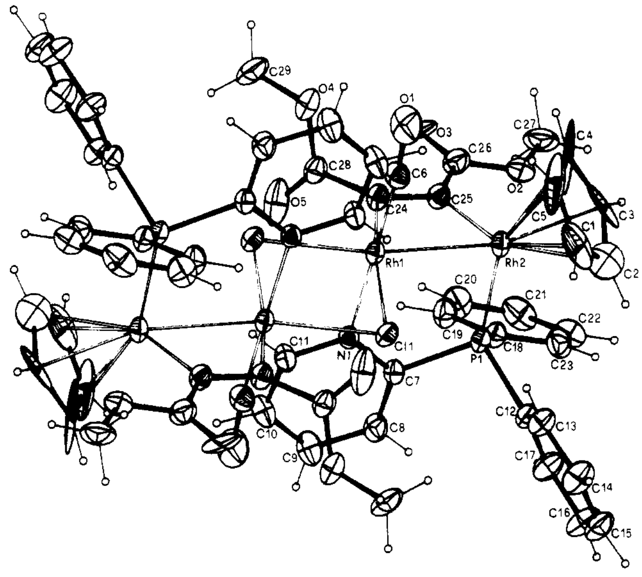

Figure 1. Perspective view of $\{[(\eta^5\text{-}C_5H_5)Rh(\mu\text{-DMA})(\mu\text{-}Ph_2Ppy)Rh(CO)(\mu\text{-}Cl)]_2\cdot CH_2Cl_2\}$ (**2**) showing the numbering scheme. The CH_2Cl_2 molecule of crystallization is omitted for clarity.

dispersion corrections for Rh, P, and Cl atoms were taken from ref 14. All calculations were performed with the SHELX76[15] and PARST[16] set of programs on the IBM 4341 computer at the "Centro di Calcolo dell'-Università di Messina". The refined structure was plotted with use of the ORTEP program. Hydrogen and non-hydrogen coordinates and anisotropic temperature factors are available as supplementary material.

Results of Synthesis

The transformations observed in this study are summarized in Scheme I.

Synthesis and Characterization of Complexes 2 and 3. Complex $[(\eta^5\text{-}C_5H_5)Rh(\mu\text{-CO})(\mu\text{-}Ph_2Ppy)Rh(CO)Cl]$ (**1**) reacts with alkynes activated by electron-withdrawing groups such as COOR (R = CH_3, C_2H_5); no reaction is observed with acetylene or diphenylacetylene under thermal conditions. The addition of an excess of dimethyl acetylenedicarboxylate (DMA) or diethyl acetylenedicarboxylate (DEA) to a dichloromethane solution of **1** leads to a rapid reaction as shown by a change of the color of the solution from red-brown to orange. Workup of the resulting solution yields the compounds **2** and **3** as shown in Scheme I. Spectral data for the new compounds are very similar. The IR spectra of **2** and **3** show terminal carbon monoxide stretching frequencies at about 2010 cm^{-1}, along with characteristic bands at 1710 and 1690 cm^{-1}, due to the ester groups, and at 1615 cm^{-1} attributable to the ν(C═C) stretch. Samples of **2** and **3** prepared from **1** containing ^{13}CO do not show any shift in the IR bands assigned to the ester groups. The ν(C═C) stretch at 1615 cm^{-1} falls at values that do not allow the two coordination modes which alkynes commonly adopt in bimetallic complexes, $\mu\text{-}\eta^2\text{-}\|$ and $\mu\text{-}\eta^2\text{-}\perp$, to be distinguished.[17-23] The X-ray crystal structure has been determined for **2**; see Figures 1 and 2. These are discussed below. Complex **2** is a tetranuclear species containing two bimetallic units linked by two chloro ligands bridging the rhodium atoms not directly involved in a metal–metal bond; each bimetallic unit contains the bridging alkyne coordinated as a cis-dimetalated olefin, $\mu\text{-}\eta^2\text{-}\|$.

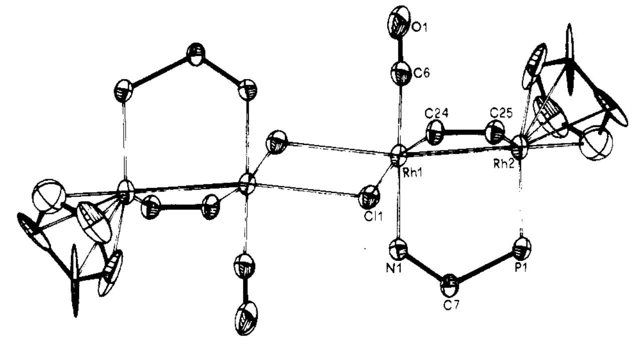

Figure 2. Inner coordination sphere of **2**.

Solution Behavior of 2. The $^{31}P\{^1H\}$ NMR spectrum of **2**, in CD_2Cl_2 solution, shows at room temperature a doublet of doublets at δ 53.4 (^1J(RhP) = 175.9, ^2J(RhP) = 4.8 Hz). When the temperature (273–253 K) is lowered, this signal broadens, and at 225 K, two sharp doublets of doublets emerge from the broad signal. These are centered respectively at δ 54.1 (^1J(RhP) = 175.6, ^2J(RhP) = 4.8 Hz) and 55.3 (^1J(RhP) = 174.9, ^2J(RhP) = 4.6 Hz). The low-temperature spectra clearly indicate the presence in solution of two different species in slow exchange on the NMR time scale. These results can be interpreted on the basis of an equilibrium between either the binuclear **4** and the tetranuclear **2** species

$$\underset{\mathbf{4}}{2[(\eta^5\text{-}C_5H_5)Rh(\mu\text{-DMA})(\mu\text{-}Ph_2Ppy)Rh(CO)Cl]} \rightleftarrows \underset{\mathbf{2}}{[(\eta^5\text{-}C_5H_5)Rh(\mu\text{-DMA})(\mu\text{-}Ph_2Ppy)Rh(CO)(\mu\text{-}Cl)]_2}$$

or between two of the possible isomers of the tetranuclear species, some of which are reported in Figure 3.

There are several possible isomers of the tetranuclear species which could be present in solution. The most likely ones are **6–8**, besides **2**. The isomerism between **2** and **6** is frequently present in halogen-bridged complexes, while the isomerism between **7** and **8** has recently been demonstrated for some palladium complexes.[24] Molecular weight measurements of **2** in CH_2Cl_2, at room temperature, over the range of concentrations 5×10^{-4} to 5×10^{-2} M gave values that are concentration dependent and indicate that the compound is extensively dissociated to the bimetallic species **4**. At the ^{31}P NMR concentration of 5×10^{-2} M, tetramer formation would be more favored, and at low temperature, formation of the tetranuclear species becomes even more favorable.

Integration of the signals of the two isomers in dichloromethane at 200 K showed that the ratio between the two isomers depends on the concentration of complex **2**. This suggests that, on the NMR time scale, a slow equilibrium between **4** (binuclear) and **2** (tetranuclear) species takes place. According to this inter-

---

(12) Cromer, D. T.; Mann, J. B. *Acta Crystallogr., Sect. A: Cryst. Phys., Theor. Gen. Crystallogr.* **1968**, *A24*, 321.

(13) Stewart, R. F. *J. Chem. Phys.* **1970**, *53*, 3175.

(14) *International Tables for X-ray Crystallography*; Kynoch: Birmingham, 1974; Vol. IV.

(15) Sheldrick, G. M. "SHELX 76 Computing System", University of Cambridge, 1976.

(16) Nardelli, M. *Comput. Chem.* **1983**, *7*, 95.

(17) Cowie, M.; Southern, T. *Inorg. Chem.* **1982**, *21*, 246 and references therein.

(18) (a) Mague, J. T. *Inorg. Chem.* **1983**, *22*, 45. (b) Corrigan, P. A.; Dickson, R. S.; Johnson, S. H.; Pain, G. N.; Yeah, M. *Aust. J. Chem.* **1982**, *35*, 2203. (c) Cowie, M.; Dickson, R. S.; Hames, B. W. *Organometallics* **1984**, *3*, 1879.

(19) (a) Dickson, R. S.; Pain, G. N.; Mackay, M. F. *Acta Crystallogr., Sect. B: Struct. Crystallogr. Cryst. Chem.* **1979**, *B35*, 2321. (b) Bennett, M. A.; Johnson, R. N.; Robertson, G. B.; Turney, T. W.; Whimp, P. O. *Inorg. Chem.* **1976**, *15*, 97.

(20) Mague, J. T.; De Vries, S. H. *Inorg. Chem.* **1982**, *21*, 1632.

(21) Mague, J. T.; Klein, C. L.; Majeste, R. J.; Stevens, E. D. *Organometallics* **1984**, *3*, 1860.

(22) Cowie, M.; Dickson, R. S. *Inorg. Chem.* **1981**, *20*, 2682.

(23) Dickson, R. S.; Kirsh, H. P. *Aust. J. Chem.* **1972**, *25*, 2535.

(24) Galli, B.; Gasparrini, F.; Mann, B. E.; Maresca, L.; Natile, G.; Manotti-Lanfredi, A. M.; Tiripicchio, A. *J. Chem. Soc., Dalton Trans.* **1985**, 1155.

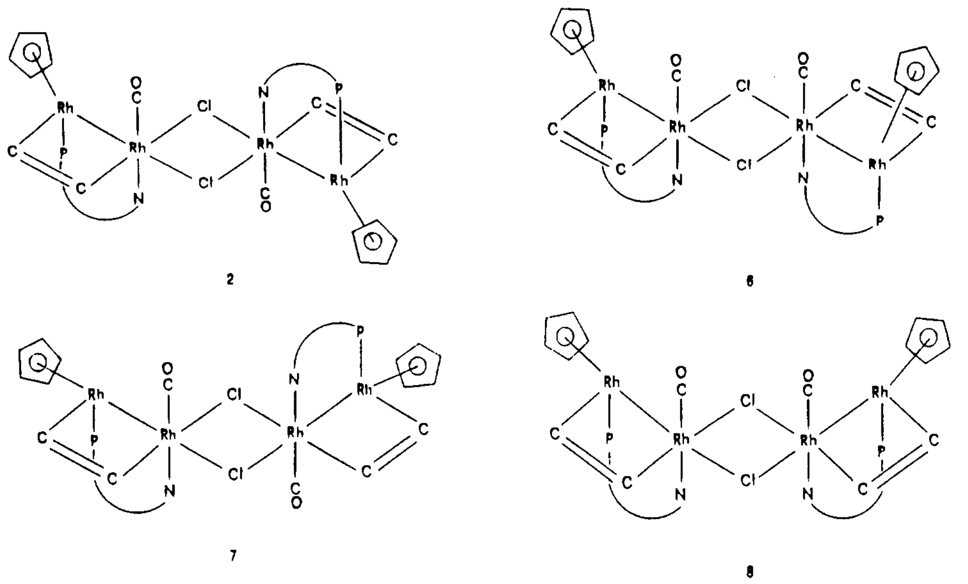

2

6

7

8

Figure 3. Some possible isomers of **2** (P⁀N = Ph_2Ppy; C=C = DMA).

pretation in the $^{31}P\{^1H\}$ NMR spectrum, the doublet of doublets at δ 54.1, which should be associated with **4**, becomes the dominant species when the concentration of 2 drops below 2×10^{-2} M; for concentrations up to 5×10^{-2} M, the doublet of doublets centered at δ 55.3, associated with the tetranuclear species, becomes dominant.

In agreement with these results, the ^1H NMR spectrum of **2**, in CD_2Cl_2, shows at room temperature a doublet of doublets for the cyclopentadienyl protons at δ 5.39 (^2J(RhH) = 0.6, ^3J(PH) = 1.9 Hz) and two different resonances for the methyl groups of the DMA moiety at δ 3.24 and 3.58. It was possible, by NOE measurements, to associate the lower frequency signal with the methyl group closer to the cyclopentadienyl and the higher frequency signal to that one closer to the α-hydrogen of the pyridine ring. At 210 K the spectrum showed the cyclopentadienyl hydrogens split into two doublets of doublets centered at δ 5.38 (^2J(RhH) = 0.6, ^3J(PH) = 1.8 Hz) and 5.41 (^2J(RhH) = 0.7, ^3J(PH) = 1.8 Hz). Again the doublet of doublets at δ 5.38 becomes the dominant species in dilute solution, while the doublet of doublets at δ 5.41 is dominant in concentrated solutions of **2**. We therefore attribute the signal at δ 5.38 to **4** and the signal at δ 5.41 to **2**.

The increase of the ^3J(PH) value for the cyclopentadienyl protons observed for **2** and **3** with respect to **1** points out that in these derivatives the formal oxidation number of the rhodium atoms is higher than in the precursor **1** and provides support for the proposal that the dimetalated olefin can be considered as a dianion.[25] In fact for the same kind of complexes the ^3J(PH) coupling constants have been related to the oxidation state of the rhodium atom in cyclopentadienyl(phosphine)rhodium complexes.[26] Considering the dimetalated olefin as a dianion,[25] the rhodium atoms in **2** and **3** are formally Rh^{II} centers; the electron count and the observed diamagnetism substantiate the presence of a metal–metal bond between the rhodium atoms bridged by the Ph_2Ppy and the acetylene ligands.

The resonances of the methyl groups of DMA in **2** are also temperature dependent. The signal at higher frequency, attributed to the methyl group closer to pyridine, is split at low temperature (210 K) into two different signals, while that at lower frequency, attributed to the methyl group closer to cyclopentadienyl, gives rise, always at the same temperature, to an unresolved single peak. Similarly the α protons on the pyridine resonances at δ 9.8 are split at 210 K into two groups of resonances, one at approximately the same δ as the signal observed at room temperature, the other shifted more than one ppm to lower frequency. This is in agreement with the hypothesis of a low-temperature induced dimerization that causes noticeable changes in the chemical environment of the 16-electron rhodium(II) center, leaving nearly unaffected the chemical environment of the 18-electron rhodium(II) center.

Reactions of 2 with CO and SO_2. We have also investigated the reactions of **2** with small molecules such as CO and SO_2 in order to verify if insertion of these species into the rhodium–rhodium or rhodium–acetylene bonds occurs. Both the reactions led to products that could not be isolated owing to the reversibility of the process. The SO_2 reaction product is stable as a solid only under an SO_2 gas atmosphere. The CO reaction products were not isolated as solids. They are detectable only in solution under a CO atmosphere. However we were able to obtain spectral information on the reaction products.

When an excess of carbon monoxide, 0.6 atm, was added to **2** at 193 K, $^{31}P\{^1H\}$ NMR spectra revealed that the starting material was completely transformed into a new product characterized by a doublet of doublets centered at δ 37.6 (^1J(RhP) = 166.6, ^2J(RhP) = 5.3 Hz). The ^{13}C NMR spectrum of the reaction mixture performed under the same experimental conditions with ^{13}C-enriched carbon monoxide showed in the carbonyl region a doublet of doublets at δ 191.0 (^1J(RhC) = 76.2, ^2J(RhC) = 4.1 Hz). The ^1H NMR spectrum of a ^{13}CO-saturated CD_2Cl_2 solution of **2** showed in the cyclopentadienyl region a doublet of doublets at δ 5.40 (^2J(RhH) = 0.6, ^3J(PH) = 1.6 Hz). These results suggest that the reaction of **2** with CO leads to an addition product. Two possible structures for this addition product are **9** and **10**. In both isomers the carbonyls are inequivalent, but one ^{13}C signal would be observed if the reaction occurred stereospecifically, placing ^{13}CO exclusively into one coordination site, or, less likely, the molecule may be highly fluxional at 193 K. Structure **10** is considered to be more probable. In fact in similar complexes the linear arrangement Rh–Rh–C, as in **9**, gives rise

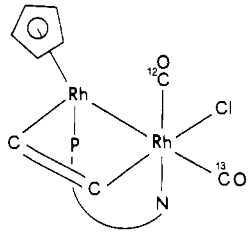

9

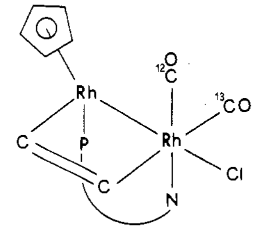

10

---

(25) Hoffman, D. M.; Hoffmann, R. *Organometallics* **1982**, *1*, 299.

(26) (a) Oliver, A. J.; Graham, W. A. G. *Inorg. Chem.* **1970**, *9*, 243, 2653; **1971**, *10*, 1165. (b) Hart-Davis, A. J.; Graham, W. A. G. *Inorg. Chem.* **1970**, *9*, 2658; **1971**, *10*, 1653. (c) Werner, H.; Feser, R. *Angew. Chem., Int. Ed. Engl.* **1979**, *18*, 158. (d) Faraone, F.; Bruno, G.; Lo Schiavo, S.; Tresoldi, G.; Faraone, G.; Bombieri, G. *J. Chem. Soc., Dalton Trans.* **1981**, 1651. (e) Faraone, F.; Bruno, G.; Lo Schiavo, S.; Tresoldi, G.; Bombieri, G. *J. Chem. Soc., Dalton Trans.* **1983**, 433.

to smaller ^1J(RhC) (~50 Hz) and more substantial ^2J(RhC) (~25 Hz) values with respect to those observed.[27] Moreover, large upfield shifts of the carbonyl resonances from the region normally associated with terminal CO have been reported for this class of complexes.[27] The same reaction performed on a sample of ^{13}C-labeled **1** allowed us to rule out the possibility of fluxionality in **10**. In this case the addition product showed besides the mentioned resonance at δ 191.0 a second resonance at δ 193 consistent with the presence of a second terminal carbonyl. The lack of resolution prevented in this case the measure of the ^2J(^{13}C^{13}C) and the ^2J(Rh^{13}C) coupling constants. The ^1J(Rh^{13}C) coupling constants for the two apparent doublets were actually equal.

Subsequently, when the sample is warmed to room temperature for 15 min, further changes in the ^{13}C and ^{31}P{^{1}H} NMR spectra occur. The most noteworthy features are the appearance of doublets at δ 211.1 (^1J(RhC) = 23 Hz) and 206.4 (^1J(RhC) = 22.5 Hz). The ^{13}C chemical shifts and J(RhC) are consistent with the formation of acyl derivatives, presumably by the insertion of ^{13}CO into a C–Rh bond.[10,11] These compounds have not been fully characterized.

The reaction of **2** with SO_2 essentially showed the same features as the reaction with CO. The addition of sulfur dioxide to **2** leads to the formation of the SO_2 adduct **11**, which is stable only under an SO_2 atmosphere. In the IR spectrum the ν(SO) stretches are observed at 1220 and 980 cm^{-1}; the former band falls at higher values than those usually reported for SO_2 bridging two metals.[28] ^{31}P{^{1}H} NMR spectra of **2** in CD_2Cl_2 saturated with SO_2 at room temperature showed formation of a doublet of doublets centered at δ 60.9 (^1J(RhP) = 162.5 Hz, ^2J(RhP) = 3.7 Hz) and complete disappearance of that at δ 54.1 present in the starting material. By analogy with the carbonyl adduct, the product could be formulated as a complex with SO_2 equatorially bonded to the rhodium atom.

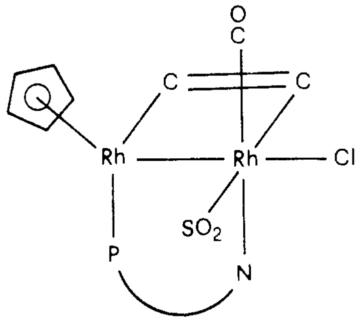

11

Crystal and Molecular Structure of {[(η^5-C_5H_5)Rh(μ-DMA)(μ-Ph_2Ppy)Rh(CO)(μ-Cl)]$_2$·CH_2Cl_2} (2). The crystal parameters of **2** are reported in Table I. The molecular structure, including the numbering scheme, is illustrated in Figure 1; the CH_2Cl_2 molecule of crystallization is omitted for clarity. A representation of the inner coordination sphere of the complex is shown in Figure 2. Final positional parameters are reported in Table II. Selected bond distances and angles are listed in Table III.

The molecule has a crystallographic inversion center relating two rhodium dimer units. Each dimer unit is completely asymmetrical and consists of two rhodium atoms bridged by Ph_2Ppy and dimethyl acetylenedicarboxylate, which has become bound as a dimetalated olefin. The cyclopentadienyl ligand completes the coordination sphere of Rh(2) while the terminal carbon monoxide and the two bridging chloride ligands complete that of Rh(1). The Rh(1)–Rh(2) bond distance of 2.661 (1) Å falls within the range expected for a single metal–metal bond[2-8,28] and is lengthened only by 0.013 Å with respect to that in **1**, as a consequence of the replacement of μ-CO by DMA. Presumably the short bite and high rigidity of 2-(diphenylphosphino)pyridine prevents significant variations in the rhodium–rhodium separation. The Rh(1)–Rh(2) distance is significantly shorter than the in-

Table II. Final Fractional Atomic Coordinates (×10^4) for **2**

atom	*x/a*	*y/b*	*z/c*
Rh(1)	664 (1)	3532 (1)	4601 (1)
Rh(2)	329 (1)	1701 (1)	2918 (1)
Cl(1)	−815 (1)	4860 (1)	3532 (1)
N(1)	2007 (3)	4377 (3)	4137 (3)
P(1)	1536 (1)	2634 (1)	2238 (1)
O(1)	−975 (4)	2241 (4)	5434 (4)
O(2)	2376 (4)	−232 (3)	3475 (3)
O(3)	3395 (5)	447 (4)	5370 (4)
O(4)	2567 (3)	2108 (3)	7161 (3)
O(5)	3714 (4)	3247 (4)	6615 (4)
C(1)	−1601 (6)	1324 (7)	1752 (10)
C(2)	−906 (8)	807 (8)	1222 (6)
C(3)	−339 (7)	−3 (6)	1854 (11)
C(4)	−688 (11)	86 (10)	2840 (10)
C(5)	−1493 (9)	908 (12)	2721 (10)
C(6)	−376 (5)	2720 (4)	5058 (5)
C(7)	2293 (4)	3990 (4)	3147 (4)
C(8)	3151 (4)	4571 (4)	2856 (5)
C(9)	3753 (5)	5558 (4)	3594 (5)
C(10)	3477 (5)	5921 (4)	4611 (5)
C(11)	2604 (4)	5328 (4)	4836 (5)
C(12)	866 (4)	3072 (4)	778 (4)
C(13)	−327 (5)	3380 (4)	464 (5)
C(14)	−884 (5)	3686 (5)	−652 (5)
C(15)	−285 (5)	3702 (5)	−1438 (5)
C(16)	907 (6)	3432 (6)	−1125 (5)
C(17)	1457 (5)	3111 (5)	−29 (5)
C(18)	2847 (4)	1843 (4)	2134 (4)
C(19)	3898 (5)	1945 (4)	3105 (5)
C(20)	4843 (5)	1274 (5)	3076 (6)
C(21)	4772 (5)	502 (5)	2085 (7)
C(22)	3726 (6)	374 (5)	1126 (6)
C(23)	2766 (5)	1030 (4)	1146 (5)
C(24)	1903 (4)	2386 (4)	5183 (4)
C(25)	1795 (4)	1513 (4)	4334 (4)
C(26)	2603 (5)	539 (5)	4477 (5)
C(27)	3147 (6)	−1178 (5)	3528 (6)
C(28)	2843 (4)	2634 (4)	6374 (4)
C(29)	3480 (6)	2184 (6)	8309 (5)
C(30)	6363 (7)	4313 (8)	1351 (8)
Cl(2)	5616 (2)	3267 (2)	1686 (3)
Cl(3)	6310 (2)	4127 (4)	9908 (3)

Table III. Selected Bond Distances (Å) and Angles (deg) for **2**

Bond Distances			
Rh(1)–Rh(2)	2.661 (1)	Rh(2)–Cp*	1.919 (9)
Rh(1)–Cl(1)	2.516 (1)	Rh(2)–P(1)	2.220 (1)
Rh(1)–Cl(1′)	2.670 (1)	Rh(2)–C(25)	2.040 (4)
Rh(1)–C(6)	1.822 (6)	C(24)–C(25)	1.310 (6)
Rh(1)–N(1)	2.133 (4)	C(6)–O(1)	1.142 (8)
Rh(1)–C(24)	2.022 (5)		
Bond Angles			
Rh(2)–Rh(1)–N(1)	95.5 (1)	Rh(1)–Cl(1)–Rh(1′)	98.1 (1)
Rh(2)–Rh(1)–C(6)	83.1 (2)	Rh(1)–Rh(2)–P(1)	86.4 (1)
Rh(2)–Rh(1)–Cl(1)	101.5 (1)	Rh(1)–C(6)–O(1)	174.7 (5)
Rh(2)–P(1)–C(18)	113.9 (2)	Rh(1)–Rh(2)–Cp*	133.6 (3)
Rh(2)–P(1)–C(7)	117.3 (2)	Rh(1)–N(1)–C(11)	119.9 (3)
Rh(2)–P(1)–C(12)	116.9 (2)	Rh(1)–N(1)–C(7)	122.6 (3)
Rh(2)–C(25)–C(24)	108.7 (4)	Rh(1)–C(24)–C(25)	109.9 (4)
Rh(2)–C(25)–C(26)	128.3 (4)	Rh(1)–C(24)–C(28)	121.4 (3)
Rh(2)–Rh(1)–C(24)	70.6 (1)	Rh(1)–Rh(2)–C(25)	70.5 (1)
Rh(2)–Rh(1)–Cl(1′)	170.1 (1)	C(6)–Rh(1)–Cl(1)	97.3 (2)
N(1)–C(7)–P(1)	117.3 (4)	C(6)–Rh(1)–Cl(1′)	87.2 (2)
N(1)–Rh(1)–C(24)	86.4 (2)	C(6)–Rh(1)–C(24)	88.2 (2)
N(1)–Rh(1)–Cl(1′)	94.1 (1)	Cl(1)–Rh(1)–Cl(1′)	81.8 (4)
N(1)–Rh(1)–C(6)	174.6 (2)	Cl(1)–Rh(1)–C(24)	169.9 (1)
N(1)–Rh(1)–Cl(1)	88.1 (1)	C(24)–Rh(1)–Cl(1′)	107.0 (1)
P(1)–Rh(2)–C(25)	87.7 (1)	P(1)–Rh(2)–Cp*	130.1 (3)

---

(27) (a) Piraino, P.; Bruno, G.; Lo Schiavo, S.; Laschi, F.; Zanello, P. *Inorg. Chem.* **1987**, *26*, 2205. (b) Lifsey, R. S.; Chavan, M. Y.; Chau, L. K.; Ahsan, M. Q.; Kadish, K. M.; Bear, J. L. *Inorg. Chem.* **1987**, *26*, 822.

(28) Kubas, G. J. *Inorg. Chem.* **1979**, *18*, 182.

(29) (a) Cowie, M.; Mague, J. T.; Sanger, A. R. *J. Am. Chem. Soc.* **1978**, *100*, 3628. (b) Cowie, M. *Inorg. Chem.* **1979**, *18*, 286 and references therein. (c) Faraone, F.; Bruno, G.; Lo Schiavo, S.; Piraino, P.; Bombieri, G. *J. Chem. Soc., Dalton Trans.* **1983**, 1819.

traligand P···N separation (2.741 (3) Å), indicating a compression along the Rh(1)–Rh(2) axis as expected for a metal–metal-bonded system. The Rh(1)···Rh(1′) separation of 3.900 (1) Å clearly indicates that these atoms are not involved in a metal–metal bond.

The structural parameters concerning the inner coordination sphere of the complex (Figure 2) support the idea that the formation of **2** occurs by an intermolecular nucleophilic attack of chlorine on the coordinatively unsaturated 16-electron rhodium(II). The attack occurs trans to the rhodium–rhodium bond. The Rh(2)–Rh(1)–Cl(1′) and Rh(2)–Rh(1)–Cl(1) bond angles of 170.1 (1) and 101.5 (3)°, respectively, are consistent with this assumption.[30] The Rh(2)–Rh(1)–Cl(1′) angle shows a deviation from linearity to minimize repulsive contacts of Cl(1′) with the pyridine ring (the Cl(1′)···N(1) and Cl(1′)···C(11) long-range interactions are 3.531 and 3.344 Å, respectively). The bond angles Rh(1)–Cl(1)–Rh(1′) and Cl(1)–Rh(1)–Cl(1′) are 98.1 (1) and 81.8 (4)°, respectively; the Rh(2) and Rh(2′) atoms lie in opposite directions, at 0.430 (1) Å out of the Rh(1)Cl(1)Rh(1′)Cl(1′) plane. In the unsymmetrical chloro bridges, both the Rh–Cl distances are somewhat long. The Rh(1)–Cl(1) bond distance of 2.516 (1) Å can be explained by the high trans influence of the σ-bonded carbon of the cis-dimetalated olefin;[17,31] the Rh(1)–Cl(1′) bond is even longer (2.670 (1) Å) and can be attributed to a higher trans influence of the rhodium–rhodium bond. Several reports indicate that a metal–metal bond produces a lengthening of the trans metal–ligand bond.[18c,30,32] The Rh(1)–Cl(1) distance is comparable with the value of 2.528 (3) Å found in the cation $[Rh_3(\mu\text{-dpmp})(\mu\text{-CO})(\mu\text{-Cl})Cl(\mu\text{-}CH_3O_2CC_2CO_2CH_3)]$ (dpmp = bis[(diphenylphosphino)methyl]phenylphosphine) in which the bridging chloride is in a position trans to the σ-bonded carbon atom of the dimetalated olefin.[33] Acetylene is attached essentially parallel to the metal–metal axis in a cis-dimetalated olefinic geometry; the acetylenic vector is twisted only by 3.8 (3)° from the metal–metal axis. Consistent with this bonding mode, the angles about the metalated carbons are reminiscent of sp^2 hybridization, and the C(24)–C(25) distance is 1.310 (6) Å, close to that of a normal carbon–carbon double bond. The DMA ligand is rather unsymmetrically coordinated, the Rh(1)–C(24) and Rh(2)–C(25) distances being significantly different (2.022 (5) and 2.040 (4) Å, respectively), and the angles around the C(24) and C(25) atoms are very different from 120°. The C(28)C(24)C(25)C(26) torsion angle is 4.4 (8)°. The methoxycarbonyl substituents are twisted with respect to each other, as generally found when DMA is bound as $\mu\text{-}\eta^2\text{-}||$.[17,34] The COOMe group bonded to C(25) lies close to the Rh(1)Rh(2)C(24)C(25) plane (7.1 (3)°) while that bonded to C(24) is nearly orthogonal with respect to the same plane (99.8°); a distorsion presumably results to minimize contacts between the methyl group bonded to O(4) and a phenyl group and between the O(5) atom and the pyridine ring [O(5)···N(7) = 3.474 Å; O(5)···C(11) = 3.481 (7) Å].

As found in similar complexes,[2-8] the cyclopentadienyl ring is located on the less hindered side of the molecule, and the bond angles at the Rh(2) atom by the centroid of the cyclopentadienyl ring (Cp*) are larger than those of other ligands. The Rh(2)–$C(C_5H_5)$ distances and the Rh(2)–Cp* separation are similar to those found in **1** and analogous rhodium–cyclopentadienyl systems.[2-8,35]

The ligands about Rh(1) are disposed in a nearly octahedral geometry. The significant deviations observed for N(1) and Cl(1) are very likely to minimize non bonded contacts between these atoms: Cl(1)···N(1) = 3.531 Å. In agreement, the N(1)–Rh(1)–Cl(1′) and N(1)–Rh(1)–Cl(1) bond angles are 94.0 (1) and 88.1 (1)°, respectively. The Rh(1)–C(6) bond distance of 1.822 (6) Å falls within the range reported for rhodium complexes containing terminal carbonyls.[36] The Rh(1)–C(6)–O(1) and Cl(1)–Rh(1)–C(6) angles of 174.7 (5) and 97.3 (2)° result from the strong nonbonded contacts between the CO groups with the cyclopentadienyl and the pyridine rings [O(1)···C(5) = 3.266 (12) Å; O(1)···C(20) = 3.660 (7) Å; O(1)···C(11) = 3.453 (7) Å]. The structural features of the bridging rigid ligand Ph_2Ppy are essentially the same as in the precursor **1**.

Discussion

It should be noted that in reaction of **1** with DMA or DEA the bridging carbonyl is ready lost and insertion of acetylenes into the metal–metal bond does not occur. Probably the small bite angle and rigidity of Ph_2Ppy prevent a nonbonding interaction between the rhodium atoms. Thus the replacement of the bridging carbonyl by acetylene is the most likely process. The structural features (Figure 2) and the solution behavior of **2** suggest that **1** reacts with DMA and DEA giving the binuclear rhodium(II) species $[(\eta^5\text{-}C_5H_5)Rh(\mu\text{-acetylene})(\mu\text{-}Ph_2Ppy)Rh(CO)Cl]$ (acetylene = DMA, **4**; acetylene = DEA, **5**), which dimerize to **2** and **3**, respectively, by formation of two chlorine bridges. In the bimetallic species **4** and **5** the rhodium atoms are different as the one bonded to η^5-cyclopentadienyl group has a coordinatively saturated 18-electron center and the other has a coordinatively unsaturated 16-electron center. Thus the unsaturated rhodium(II) atom in **4** and **5** is available for nucleophilic attack along the rhodium–rhodium axis;[37] it may easily bind an additional chloride by an intermolecular process, giving **2** and **3**. The unsaturation of the 16-electron rhodium plays an important role in the reactivity of these complexes. It accounts for the formation of the tetranuclear species and for the reactions with small molecules such as SO_2 and CO.

As concerns the reactions of **2** with CO and SO_2, a remarkable feature is the lack of formation of products containing these small molecules inserted into the rhodium–rhodium bond. Such a reaction has been reported[18c] for the complexes $[Rh_2X_2(\mu\text{-acetylene})(dppm)]_2$ (X = Cl, I; acetylene = $F_3CC_2CF_3$, DMA). Very likely the different pathway observed may be attributed to the different characteristics of the Ph_2Ppy and dppm ligands and the effects that these have on the rhodium–rhodium bond.

Acknowledgment. We thank the CNR (Rome) and the Public Education Ministry for financial support.

Registry No. **1**, 119326-23-7; **2**, 121072-51-3; **3**, 121030-85-1; **10**, 121030-86-2; **11**, 121055-39-8; CO, 630-08-0; SO_2, 7446-09-5; Rh, 7440-16-6.

Supplementary Material Available: Tables listing crystallographic parameters, anisotropic and isotropic thermal parameters for non-H atoms, fractional atomic coordinates for H atoms, and complete bond lengths and angles (4 pages); a table of structure factors (24 pages). Ordering information is given on any current masthead page.

---

(30) Cotton, F. A.; Dumbar, K. R. *J. Am. Chem. Soc.* **1987**, *109*, 3142 and references therein.

(31) (a) Cowie, M.; Ibers, J. A. *Inorg. Chem.* **1976**, *15*, 552. (b) Itoh, K.; Matsuda, I.; Veda, F.; *J. Am. Chem. Soc.* **1975**, *97*, 4748. (c) Itoh, K.; Matsuda, I.; Veda, F.; Ishii, Y.; Ibers, J. A. *J. Am. Chem. Soc.* **1977**, *99*, 2118.

(32) (a) Cowie, M.; Gibson, J. A. *Organometallics* **1984**, *3*, 984. (b) Farr, J. P.; Olmstead, M. M.; Balch, A. L. *Inorg. Chem.* **1983**, *22*, 1229.

(33) Balch, A. L.; Fosset, L. A.; Linehan, J.; Olmstead, M. M. *Organometallics* **1986**, *5*, 691.

(34) Cowie, M.; Southern, T. G. *J. Organomet. Chem.* **1980**, *193*, C46.

(35) (a) Mills, M. S.; Paulus, E. F. *J. Organomet. Chem.* **1967**, *10*, 331. (b) Herrmann, W. A.; Bauer, C.; Kriechbaum, G.; Kunkely, H.; Ziegler, M. L.; Speth, D.; Guzzolz, E. *Chem. Ber.* **1982**, *115*, 878. (c) Herrmann, W. A.; Goddard, C. K. R.; Bernal, I. *J. Organomet. Chem.* **1977**, *140*, 73.

(36) (a) Colton, R.; Mc Cormick, M. J. *Coord. Chem. Rev.* **1980**, *31*, 1. (b) Cotton, F. A. *Prog. Inorg. Chem.* **1976**, *21*, 1.

(37) (a) Cotton, F. A.; Walton, R. A. *Multiple Bonds Between Metal Atoms*; Wiley: New York, 1982. (b) Felthouse, T. R. *Prog. Inorg. Chem.* **1982**, *29*, 73.